Mechanistic Implications of the Structure of the Mixed-Disulfide Intermediate of the Disulfide Oxidoreductase, 2-Ketopropyl-Coenzyme M Oxidoreductase/Carboxylase[†,‡]

Arti S. Pandey,[§,||] Boguslaw Nocek,[§,||] Daniel D. Clark,[⊥] Scott A. Ensign,[⊥] and John W. Peters*[,||]

Department of Chemistry and Biochemistry, Montana State University, Bozeman, Montana 59717, and Department of Chemistry and Biochemistry, Utah State University, Logan, Utah 84322

Received July 29, 2005; Revised Manuscript Received November 1, 2005

ABSTRACT: The structure of the mixed, enzyme-cofactor disulfide intermediate of ketopropyl-coenzyme M oxidoreductase/carboxylase has been determined by X-ray diffraction methods. Ketopropyl-coenzyme M oxidoreductase/carboxylase belongs to a family of pyridine nucleotide-containing flavin-dependent disulfide oxidoreductases, which couple the transfer of hydride derived from the NADPH to the reduction of protein cysteine disulfide. Ketopropyl-coenzyme M oxidoreductase/carboxylase, a unique member of this enzyme class, catalyzes thioether bond cleavage of the substrate, 2-ketopropyl-coenzyme M, and carboxylation of what is thought to be an enzyme-stabilized enolacetone intermediate. The mixed disulfide of 2-ketopropyl-coenzyme M oxidoreductase/carboxylase was captured through crystallization of the enzyme with the physiological products of the reaction, acetoacetate, coenzyme M, and NADP, and reduction of the crystals with dithiothreitol just prior to data collection. Density in the active-site environment consistent with acetone, the product of reductive decarboxylation of acetoacetate, was revealed in this structure in addition to a well-defined hydrophobic pocket or channel that could be involved in the access for carbon dioxide. The analysis of this structure and that of a coenzyme-M-bound form provides insights into the stabilization of intermediates, substrate carboxylation, and product release.

The NADPH:2-ketopropyl-coenzyme M (CoM)[1] carboxylase/oxidoreductase (2-KPCC) catalyzes the reductive cleavage and carboxylation of 2-ketopropyl-CoM (2-KPC) to produce acetoacetate and free CoM (*1*, *2*) as shown in eq 1

$$\text{2-ketopropyl-CoM} + \text{NADPH} + \text{CO}_2 \rightarrow \text{acetoacetate} + \text{NADP}^+ + \text{CoM} \quad (1)$$

This reaction is the final step in a bacterial pathway by which aliphatic epoxides such as epoxypropane are converted to β keto acids for entry into central metabolic pathways (*3*−*6*).

The stoichiometry of this reaction and the molecular properties of 2-KPC reveal a fundamentally new type of chemistry and associated mechanism for the carboxylation of an organic substrate, without precedent for all other known carboxylases (*7*−*10*). The biochemical (*1*, *3*, *4*, *11*) and structural features (*12*) of 2-KPCC have shown that the enzyme is a member of the disulfide oxidoreductase (DSOR) family of enzymes (*13*) (Figure 1A) (*12*), which includes such well-characterized enzymes as glutathione reductase (*14*−*16*), mercuric reductase (*17*), and dihydrolipoamide dehydrogenase (*18*). Mechanistic studies of 2-KPCC have provided evidence that the cleavage of 2-ketopropyl-CoM is facilitated by attack of the distal (interchange) thiol (Cys82) on the thioether bond of 2-KPC, forming a mixed disulfide of CoM and Cys82 as shown in Figure 1B (*1*). The other product of thioether bond cleavage, enolacetone, is subsequently carboxylated to form the product acetoacetate. The mixed disulfide of CoM and Cys82 is then reduced by formation of a disulfide between Cys82 and the flavin thiol Cys87. NADPH then reduces the disulfide bond between Cys82 and Cys87 via flavin mediation as observed for other DSOR enzymes (*19*). At present, 2-KPCC is the only known member of the DSOR family to catalyze thioether bond cleavage and organic substrate carboxylation.

The three-dimensional structure of 2-KPCC has been solved by X-ray crystallography, both in the absence and presence of the substrate 2-KPC (*12*). Relative to other

[†] This work was supported by the Department of Energy Grant DE-FG02-04ER15563 (to J.W.P.) and National Institutes of Health Grant GM51805 (to S.A.E.). Portions of this research were carried out at the Stanford Synchrotron Radiation Laboratory, a national user facility operated by Stanford University on behalf of the U.S. Department of Energy, Office of Basic Energy Sciences. The SSRL Structural Molecular Biology Program is supported by the Department of Energy, Office of Biological and Environmental Research, and by the National Institutes of Health, National Center for Research Resources, Biomedical Technology Program, and the National Institute of General Medical Sciences.

[‡] Coordinates for the structure of mixed-disulfide- and CoM-bound states of 2-KPCC have been deposited in the Protein Data Bank as entries 2c3c and 2c3d, respectively.

* To whom correspondence should be addressed. Telephone: 406-994-7211. Fax: 406-994-7212. E-mail: john.peters@chemistry.montana.edu.

[§] These authors contributed equally to this work.

[||] Montana State University.

[⊥] Utah State University.

[1] Abbreviations: FAD, flavin adenine dinucleotide; NADP, nicotinamide adenine dinucleotide phosophate; CoM, coenzyme M (2-mercaptoethanesulfonate); 2-KPC, 2-ketopropyl-CoM; 2-KPCC, NADP-dependent 2-ketopropyl-CoM oxidoreductase/carboxylase; DSOR, disulfide oxidoreductase.

10.1021/bi051518o CCC: $33.50
Published on Web 12/08/2005

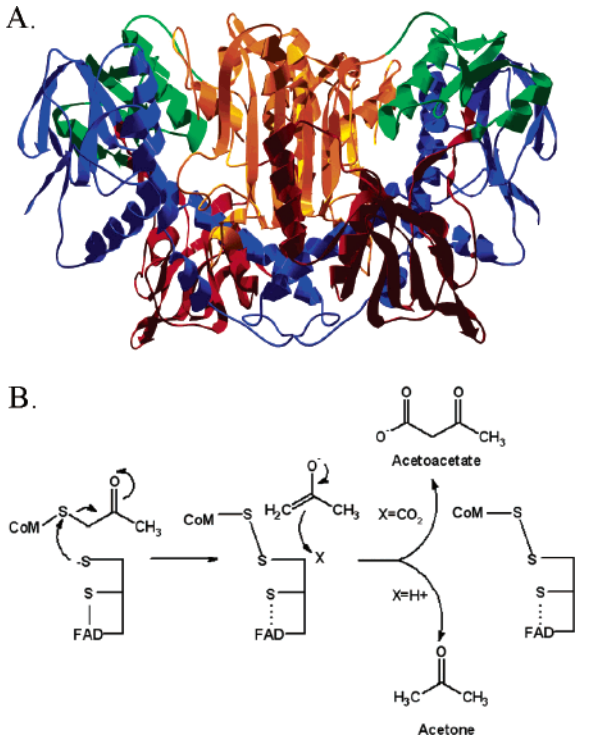

FIGURE 1: (A) Ribbon representation of the homodimeric 2-KPCC (PDB code 1MO9) showing FAD-binding (brown), NADP-binding (blue), central (green), and interface (orange) domains. (B) Summary of 2-KPCC-catalyzed acetoacetate and acetone formation both occurring via the formation of a mixed-disulfide and stable enolate intermediate.

DSOR enzymes, 2-KPCC has an extended N-terminus and a 13 amino acid insertion within the interface domain that effectively eliminates the larger cleft providing access to the active site for other members of this family. In the substrate-bound form, 2-KPC is oriented in the active site such that there is a linear pathway for electron pair transfer between flavin adenine dinucleotide (FAD), the redox-active disulfide, and the thioether bond of the substrate. The sulfonate of 2-ketopropyl-CoM forms a salt bridge with two specific Arg residues. The carbonyl of the substrate is located within hydrogen-bonding distance of an ordered water molecule that might donate a proton for stabilization of enolacetone. The remainder of the active-site environment is largely hydrophobic. Together, these unique features of the 2-KPCC active site are believed to facilitate the sequestration of enolacetone to promote carboxylation rather than protonation, an undesirable side reaction producing acetone as a dead-end product.

To shed further light on the mechanism of 2-KPCC, we have, in the present work, established conditions for crystallizing the enzyme in a state where the mixed disulfide between CoM and Cys82 can be directly visualized, thereby providing direct evidence for the existence of this novel intermediate in the reaction pathway. Along with structural studies of a CoM-bound form of the enzyme, these studies provide new insights into the mechanism of thioether bond cleavage and substrate carboxylation catalyzed by this atypical member of the DSOR family.

EXPERIMENTAL PROCEDURES

Xanthobacter autotrophicus (strain Py2) cells were grown as previously described (*20*), and 2-KPCC was purified according to the method described previously (*4*). Initial attempts at obtaining crystals of the mixed-disulfide state of 2-KPCC using the previously characterized crystals (*21*) used to determine the substrate-bound state by the addition of the reductant prior to data collection were unsuccessful. Subsequent attempts consisted of screening all available crystal form by adding exogenous reductant for defined time periods prior to data collection. It was discovered that the mixed disulfide could be observed when the reductant was added to crystals that were obtained when acetoacetate, CoM, and $NADP^+$ were added prior to crystallization. One possible explanation for this is that the mixed disulfide can only be obtained in the presence of NADP(H) as an electron-transfer conduit for the reduction of the redox-active disulfide. The crystals for this study were obtained by incubating purified 2-KPCC (~30 mg/mL) with acetoacetate, CoM, and NADPH for 10 min prior to the addition of an equal amount of precipitating solution of 0.1 M ammonium acetate, 0.085 M sodium citrate at pH 5.6, 25% PEG 4000, and 30% glycerol. Drops of this mixture were allowed to incubate as hanging drops on siliconized slides with a reservoir of 0.8 mL of the above precipitating solution. As observed previously for crystals grown in the presence of the substrate 2-ketopropyl-CoM, flat rectangular crystals appeared in 3 days and continued to grow to a maximum length of 0.5 mm. The crystals obtained belong to monoclinic space group $P2_1$ with one dimer per asymmetric unit with the following unit cell dimensions: $a = 88.1$ Å, $b = 60.0$ Å, $c = 105.9$ Å, and $\beta = 102.4°$. Capturing the mixed-disulfide NADP(H)-bound state of 2-KPCC required the incubation of these crystals with 10 mM dithiothreitol (DTT) dissolved in the crystallization mother liquor for 10 min prior to cryo-preserving the crystals by plunging in liquid nitrogen. Data were collected at SSRL beamline 9-1 equipped with a mar345 imaging plate detector (marUSA, Inc.) with 1° oscillations.

Crystals of CoM-disulfide-bound 2-KPCC were obtained by incubating purified protein samples (~30 mg/mL) with 20 mM CoM prior to crystallization. Crystals were obtained by vapor diffusion using a precipitating solution consisting of 0.17 M sodium acetate, 0.085 M Tris-HCl at pH 8.5, 25.5% (w/v) poly(ethylene glycol) 4000, and 15% (v/v) glycerol and cryo-cooled in liquid nitrogen before data collection as described previously (*21*) These crystals also belonged to the monoclinic space group $P2_1$ with one dimer per unit cell of dimensions $a = 87.8$ Å, $b = 60.1$ Å, $c = 105.6$ Å, and $\beta = 99.9°$.

The data were processed with MOSFLM (*22*) and scaled with SCALA of the CCP4 program suite (*23*). Because crystals of 2-KPCC grown in the presence of CoM or CoM and acetoacetate belonged to the same space group with unit cell dimensions similar to those of the substrate-bound enzyme ($a = 88.0$ Å, $b = 60.1$ Å, $c = 105.6$ Å, $\beta = 102.5°$) with one dimer per asymmetric unit, the substrate-bound structure (1MO9) required limited repositioning for initial refinement of these structures using CNS (*24*). Improvement of the structures was accomplished by iterative model building in O (*25*) using sigma A weighted $2F_o - F_c$ maps calculated with CNS. The structures were refined to the full resolution of usable data for the two data sets from 50 to 2.15 Å and 50 to 2.15 Å resolutions for the mixed-disulfide- and CoM-disulfide-bound 2-KPCC models, respectively. A

Table 1: 2-KPCC Data and Refinement Statistics

data collection statistics	mixed disulfide	CoM disulfide
resolution (Å)	2.15	2.15
number of observed reflections	218 816	226 112
number of unique reflections	62 300	65 514
R_{merge}[a] (%)	9.3 (23.8)	8.3 (36.8)
completeness (%)	95.1 (82.8)	97.8 (76.4)
I/σ	5.5 (2.5)	7.6 (1.9)
data statistics for the highest resolution shell indicated in parentheses		
refinement statistics		
resolution range (Å)	20.0−2.15	20.0−2.15
R_{cryst} (%)	17.7	19.2
R_{free} (%)	22.6	23.6
number of non-hydrogen atoms		
protein	8046	8046
cofactor/substrate	224	127
solvent	710	698
rmsd from target values		
bond lengths (Å)	0.008	0.006
bond angles (deg)	1.440	1.290
average B factors (Å^2)		
protein main chain	21.7	21.3
protein side chain	23.7	22.3
FAD	19.2	21.4
NADP	35.5	
2-ketopropyl-CoM		
acetone	29.9	
CoM	20.6	
HOH	31.6	39.9
CoM-CoM		34.4

[a] $R_{merge} = \sum_{hkl}\sum_i|I_i - \langle I\rangle|/\sum_{hkl}\sum_i|\langle I\rangle|$, where I_i is the intensity for the ith measurement of an equivalent reflection with indices h, k, and l.

1σ cutoff was applied to the data in the latter stages of the refinement.

The results of the refinement for all structures are given in Table 1. The final structural models obey reasonable stereochemistry, with 100% of the residues occupying allowed regions of the Ramachandran plot calculated using PROCHECK (*26*). Electron-density and superimposition figures were generated using SWISSPDB VIEWER (*27*). Surface-rendering figures were generated with SPOCK (*28*). Chemical-pathway figures were created with the software ACD/CHEMSKETCH (*29*).

RESULTS AND DISCUSSION

The Mixed-Disulfide State. The proposed mechanism of 2-KPC reduction and carboxylation assumes the formation of a mixed disulfide between the interchange thiol (Cys82) and CoM (Figure 1B) (*1*). The mixed-disulfide state of glutathione reductase has been successfully captured, and a 2.0 Å structure of this state has been determined providing insights into the thiol-catalyzed reductive cleavage of the disulfide of the substrate (*14*).

We have been able to capture the mixed-disulfide state in protein crystals of 2-KPCC, and the structure of this state of the enzyme has been determined and refined to near 2.0 Å resolution. A number of unsuccessful attempts were made at stably capturing this intermediate state by the reduction of crystals grown in the presence of CoM prior to data collection. The mixed-disulfide state was obtained by growing crystals in the presence of physiological products of the reaction, acetoacetate, CoM, and $NADP^+$. Incubation of the crystals grown under these conditions with DTT for 10 min prior to data collection resulted in the stabilization of a high population of the mixed-disulfide state. This mixed disulfide is well-defined in the electron-density maps (Figure 2). Although NADP(H) is clearly visible in the electron-density maps, density consistent with the presence of intact acetoacetate is not observed. In lieu of acetoacetate, density consistent with acetone, the product of acetoacetate decarboxylation, is observed at a site approximately 4.5 Å from the sulfur atoms of the disulfide. This electron-density feature would also be consistent with acetate, which is a component of the crystallization solution. However, density is not observed at this position in the native 2-KPCC (without substrates or products bound), and the structure of native 2-KPCC was determined from crystals that were also grown in the presence of acetate. It is reasonable that, during the course of crystallization or during the incubation with DTT, acetoacetate was reductively decarboxylated to form acetone and carbon dioxide, a previously reported 2-KPCC-catalyzed reaction (*1*). Unambiguous density consistent with CO_2 as a product of this reaction is, however, not observed. The binding mode of the acetone or acetate ion at the enzyme active site has some interesting implications on potential mechanisms for product formation and release that will be discussed in detail below.

The binding of the sulfonate moiety of CoM is analogous to the substrate-bound state (Figure 3A), primarily because of interactions with Arg56 and Arg365 at the active site. In our previous work (*12*), we have extensively characterized the substrate-bound state of 2-KPCC and suggested that a well-defined enclosed substrate-binding pocket composed of largely hydrophobic amino acid residues was a critical factor in discriminating between protons and CO_2 and favoring physiologically relevant carboxylation and acetoacetate formation. In Figure 3B, the substrate is bound at the active site in a manner such that a His-oriented water molecule is interacting directly with the carbonyl group of the ketopropyl moiety of 2-KPC. We have suggested that this water molecule could be involved in the formation and stabilization of enolacetone, generating a suitable nucleophile for the reaction with an electrophilic substrate such as a proton or carbon dioxide. These interactions poise the keto-propyl moiety of 2-KPC almost directly opposite of the sulfur of the attacking Cys residue in an appropriate orientation for a leaving group. In this mode of substrate binding, the site of the proposed formation of the enolacetone intermediate (Figure 1B) is largely hydrophobic, and we have suggested that the exclusion of the solvent at this site is a key factor in promoting carboxylation over protonation. In the structure of the mixed-disulfide state, the pocket, which bound the keto-propyl moiety, is no longer occupied and it appears that the water molecule, which was previously bound at His137, has migrated to within hydrogen-bonding distance of the thiol sulfur of CoM (Figure 3C). This water molecule is now poised to protonate the free CoM product upon reoxidation of the enzyme disulfide.

Structural Changes in the Substrate-Binding Site. As previously mentioned, the binding of the substrate to 2-KPCC induces a conformational change that results in the sequestration of the substrate at the dimer interface in an environment that favors carboxylation and the formation of acetoacetate (*12*). The residues that are involved in this conformation change are predominantly in the region of the N-terminus

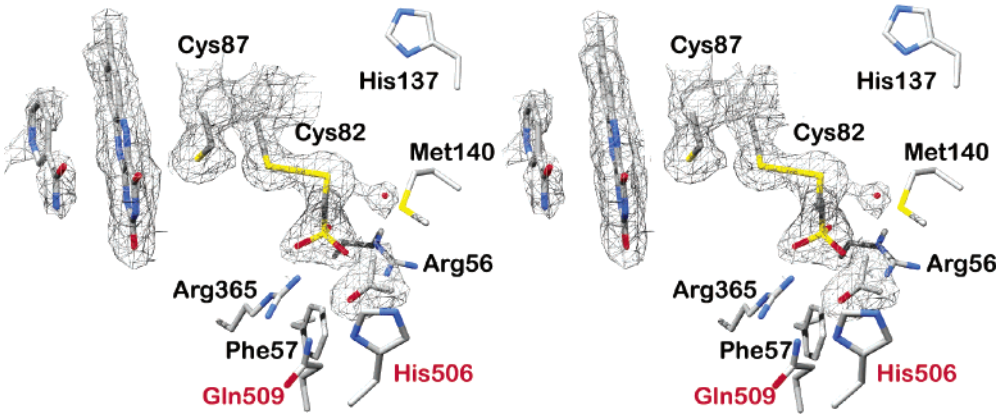

FIGURE 2: Stereoview of the active site of the mixed-disulfide-bound state of 2-KPCC with electron-density maps ($2F_o - F_c$) of the 2-KPCC mixed-disulfide state contoured (1σ) around NADP, FAD, Cys87, Cys82-CoM, and acetone.

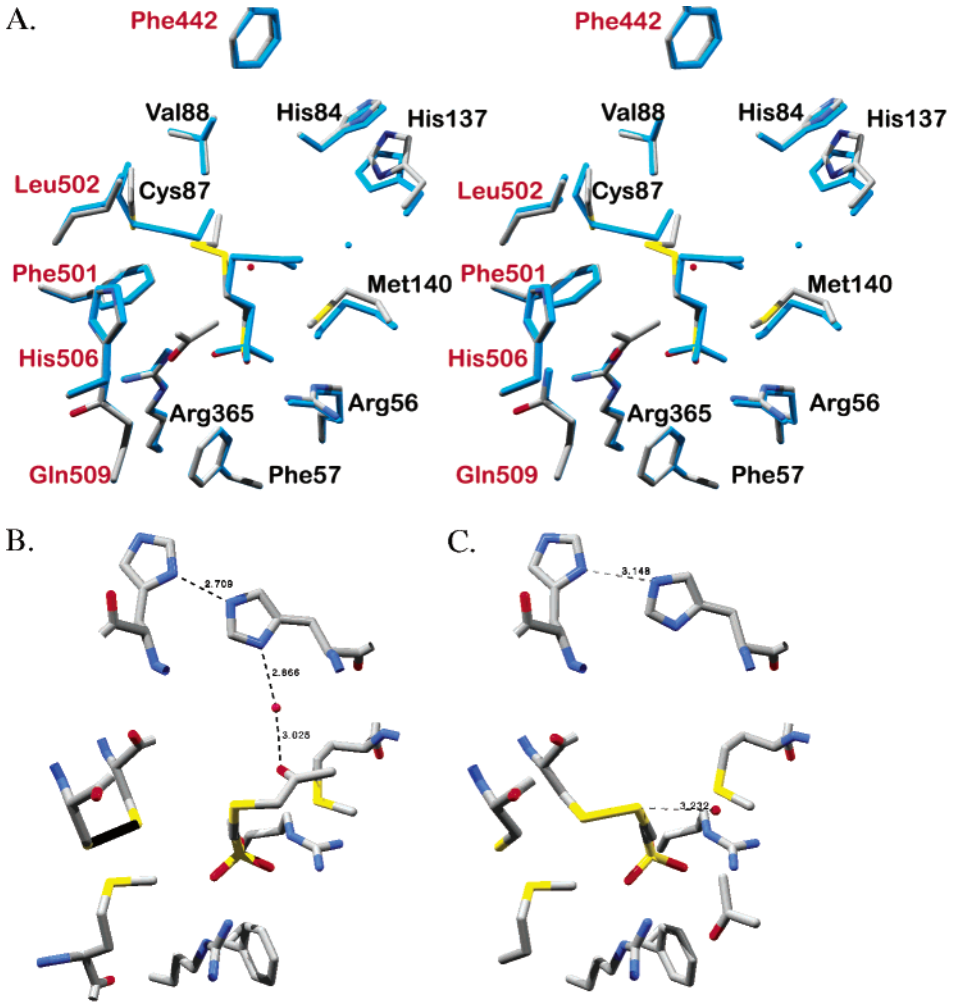

FIGURE 3: (A) Stereoview of the superimposition of the substrate-binding-site residues of Cys82-CoM mixed disulfide and acetone-bound structure (CPK) on KCoM-bound 2-KPCC (cyan). Residues from different subunits of the dimer are indicated in black and red labels. (B) Structural representations of substrate binding in the previously characterized 2-KPCC substrate-bound state (PDB code 1MO9) showing the redox-active disulfide, bound substrate, and His-oriented water molecule previously suggested to be involved in enolate formation/stabilization and the same region in the mixed disulfide between 2-KPCC Cys82 and CoM (C).

and the region of the His residue previously implicated in having a role in enolacetone formation/stabilization. These observations support the idea that substrate binding induces a structural change in the N-terminus of 2-KPCC that leads to modulation of the substrate access channel, restricting the accessibility of the bulk solvent to the channel. Interestingly, when the substrate-bound state is superimposed onto the mixed-disulfide state, very few differences are observed in the active-site region (Figure 3A). Only a slight movement of the Cys 82 side chain is required for formation of the mixed disulfide. The one significant difference that is clear in the active site in comparing these states is the position of the side chain of His137. In the substrate-bound state, this His is hydrogen-bonded to a water molecule that is in turn hydrogen-bonded to the substrate carbonyl group. In the mixed disulfide, this water molecule is absent and the side

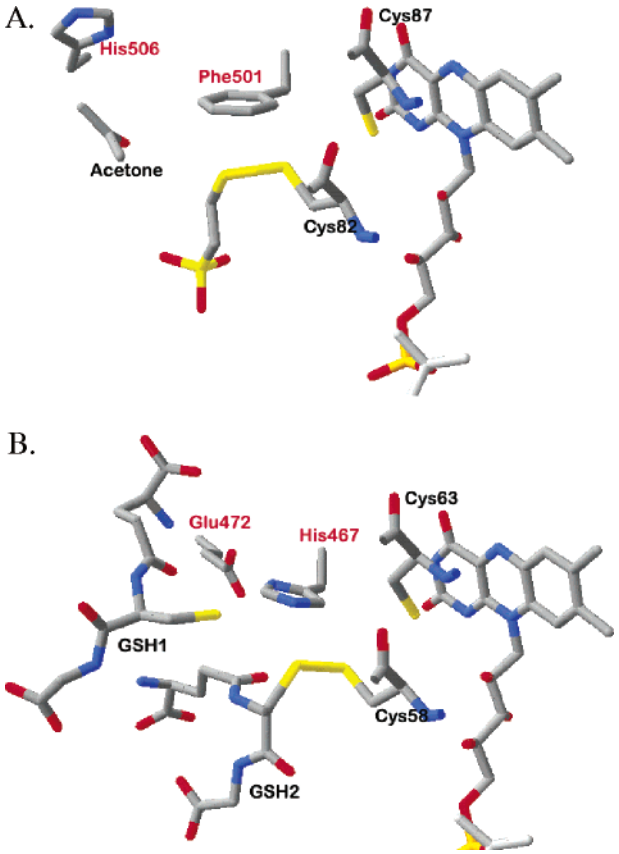

FIGURE 4: Comparison of the mixed-disulfide states of 2-KPCC (A) and glutationine reductase [PDB code 1GRE (*14*)] (B) highlighting the position of the initial leaving groups, acetone and glutathione, for 2-KPCC and GR, respectively.

chain of His137, which has been proposed to be involved in substrate binding and enolate stabilization, rotates away from the active-site cavity.

Electron density consistent with acetone/acetate was clear in the substrate-binding pocket approximately 4.5 Å away from the sulfur of CoM. Binding of acetone/acetate is stabilized by a specific hydrogen-bonding interaction (~3 Å) between the carbonyl group oxygen and the amide nitrogen of the side chain of Gln509 of the opposing subunit. In addition to being the product of reductive decarboxylation of acetoacetate, acetone is the product of the 2-KPCC reductive cleavage of 2-KPC in the absence of CO_2. Acetone as a leaving group during reductive cleavage of 2-KPC (Figure 4A) is in a similar relative position to the position of the reduced glutathione leaving group in the reductive cleavage of glutathione disulfide (Figure 4B) in glutathione reductase (GR) (*14*). Figure 4 also shows the positions of the catalytic dyad of GR, which consists of His467 and Glu472 in a conserved motif (HXXXXE) among the many DSOR enzymes. These residues are contributed by the subunit opposite the subunit contributing the redox-active disulfide. It has been proposed that this catalytic dyad in these enzymes facilitates catalysis by specific protonation of the initial leaving group by His (*13*), His467 in the case of *Escherichia coli* GR (*14*). In 2-KPCC, this DSOR motif is not conserved and is replaced by FLNPTH, and thus, a Phe replaces the His observed in many DSOR enzymes. This difference is a likely reflection of the different chemical reactions catalyzed by the DSOR enzyme, like GR and 2-KPCC. In GR, protonation of the leaving group is important for enzyme turnover to the productive product reduced glutathione. In 2-KPCC, protonation of the leaving group of reductive carbon sulfur bond cleavage is not desirable and instead carboxylation leads to the productive product acetoacetate. Thus, the absence of this protonatable group in the active site may be very important for promoting carboxylation of the enolacetone intermediate and acetoacetate formation over protonation and acetone formation. There are no charged residues around the charge-transfer thiol Cys87 that can be assigned a role in facilitating an attack on the enzyme-CoM mixed disulfide in 2-KPCC, and we have suggested above that perhaps a water molecule that can only come into proximity of the active-site Cys thiol after dissociation of the leaving group might be serving this role.

Potential CO_2 Channel. 2-KPCC catalyzes the reductive cleavage and carboxylation of a β ketothioether to form a β keto acid. It also catalyzes the reverse reaction, which is the decarboxylation of the product acetoacetate, to form 2-KPC and CO_2 in the presence of nicotinamide adenine dinucleotide phosophate (NADP) and CoM (*1*). In the absence of CO_2, protonation of the proposed enolate intermediate occurs, resulting in the formation of acetone, which is not a substrate for 2-KPCC. The characteristically hydrophobic region in the active site could be a possible binding site for CO_2. A CO_2 docking into this active site shows the molecule to be bound at the subunit interface just like the substrate and the other product acetone. A surface rendering of the region shows that CO_2 bound at this site is visible from the surface and is possibly the way in/out for CO_2 (Figure 5A). This potential channel for the CO_2 access is composed of hydrophobic residues from both subunits (Figure 5B).

With regard to the active species used by 2-KPCC, CO_2 rather than bicarbonate is believed to be the substrate for the enzyme, as assumed in the discussion above. Initial rate studies using CO_2 versus bicarbonate as a substrate suggest this as well as ^{14}C fixation studies using $^{14}CO_2$ and $NaH^{14}CO_3$ as a substrate (J. M. Boyd, J. W. Peters, and S. A. Ensign, unpublished results). 2-KPCC does not require biotin or ATP, which are required for enzymatic activation of bicarbonate as an electrophile in enzymes that use bicarbonate as the active species, providing further support for the idea that CO_2 is the active species for 2-KPCC.

Genetic-structural studies in the case of human carbonic anhydrase have indicated that a hydrophobic pocket is required for substrate (CO_2) association (*30*, *31*). Although the conservation of a well-defined pocket in human carbonic anyhydrase is critical for proper substrate association, a deeper pocket does not severely hinder efficient catalysis, but a shallower pocket results in a 3×10^5-fold loss of CO_2 hydrase activity (*31*). As stated for carbonic anhydrase, the hydrophobic pocket is probably involved in desolvation of the substrate as well as funneling the substrate toward the active site, and a variety of surface contours will satisfy this role as long as minimal requirements of pocket width and depth are met (*32*). The potential CO_2-binding pocket of 2-KPCC possesses the aforementioned features in terms of the nature of the constituent amino acids as well as the location of the pocket. The CO_2-binding hydrophobic pocket is adjacent to the acetone/acetate-binding site and is formed primarily from side chains of hydrophobic residues (Figure 5B). These include Ala17, Pro136, Ile139, Val88, Pro89, and Phe93 from one subunit. The residues from the other subunit

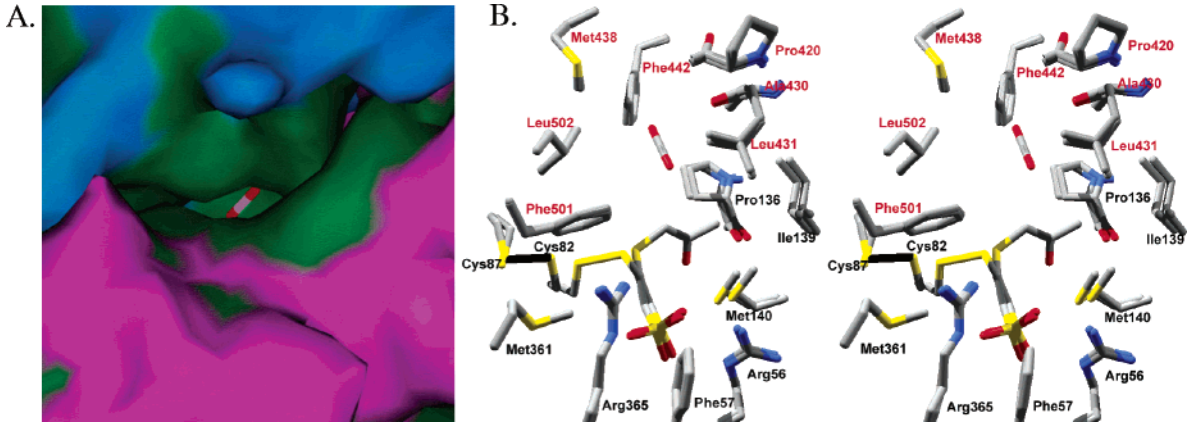

FIGURE 5: (A) Surface rendering of potential CO_2 access channel generated using SPOCK, showing a CO_2 molecule docked into the hydrophobic pocket of the substrate-binding site. Hydrophobic surfaces are shown in green. (B) Stereoview of the superimposition of the substrate- and mixed-disulfide-bound states of 2-KPCC, showing selected amino acid residues of the hydrophobic portion of the substrate-binding pocket.

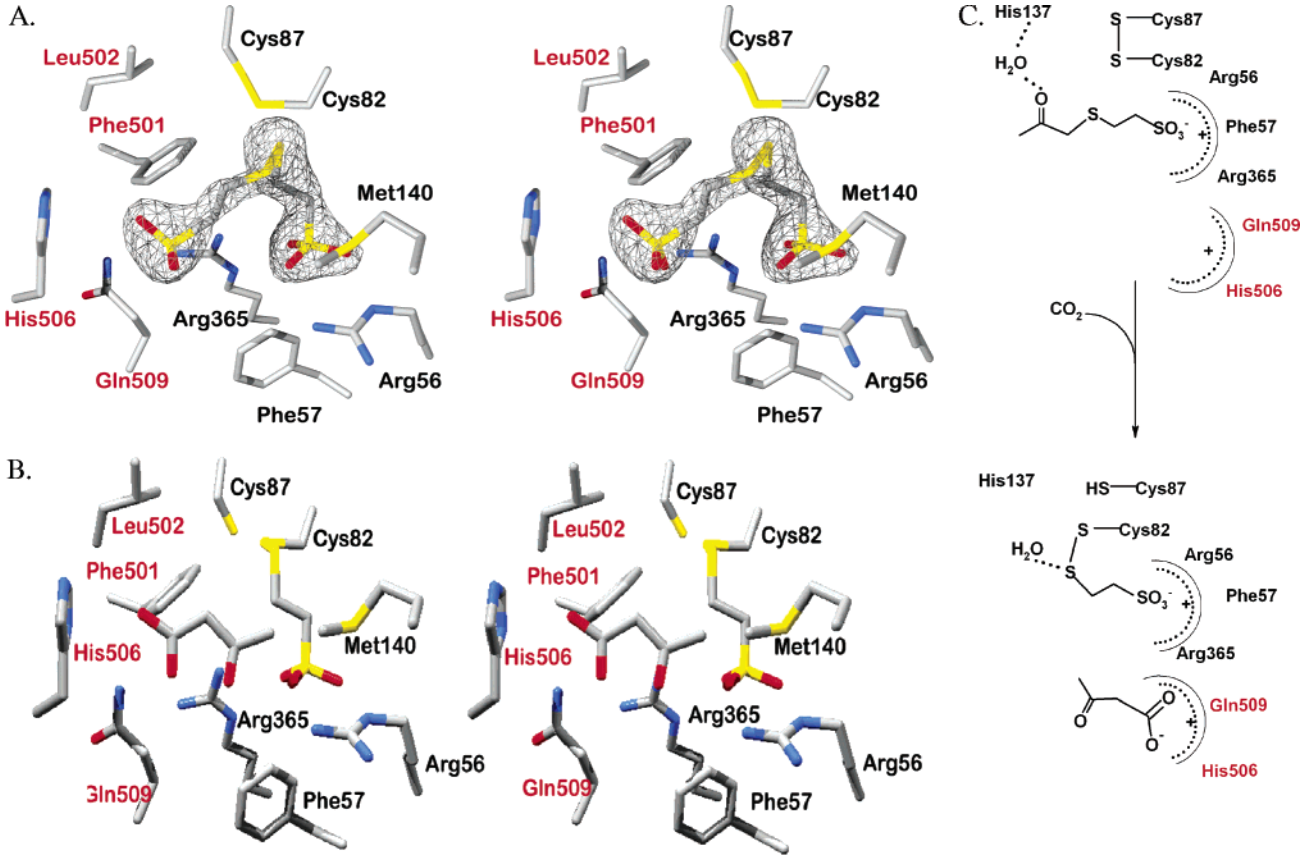

FIGURE 6: (A) $2F_o - F_c$ electron-density maps of the CoM 2-KPCC structure contoured (1σ) about the bound CoM disulfide. (B) Acetoacetate modeled into the alternative anion-binding site based on the position of the sulfonate oxygens (carboxylate of acetoacetate positioned at the site of sulfonate of CoM disulfide) in the CoM-bound structure and the position of acetone in the mixed-disulfide structure. (C) Schematic representation of the hypothetical mechanism of product formation/stabilization in 2-KPCC.

are contributed by the residues of a proline-flanked loop region unique among the DSOR enzymes to 2-KPCC and include Ala430, Leu431, Ala433, and Ser434, with the Cα of this Ser facing the CO_2-binding cavity. Phe501 and a *cis* Leu502 of the FLNPTH sequence and Phe442 from the interface domain of the other subunit are the residues forming the rest of the CO_2-binding pocket (Figure 5B).

Product Binding and Release. The structure of 2KPCC obtained from cocrystallization of the enzyme with CoM reveals CoM disulfide at the active site (Figure 6A). Although freshly prepared CoM thiol was added to the protein prior to crystallization, it appears that, during the 2−3-week-long period of incubation at room temperature in air required for crystallization, the CoM has oxidized to form CoM disulfide. This CoM disulfide binds primarily through interactions between its sulfonate moiety with active-site residues of both of the subunits. In an earlier work (*2*), 1,3-propane dithiol (PDT) has been shown to reduce 2-KPCC in the presence of $NADP^+$. The reduction of the enzyme by PDT is entirely dependent upon the presence of $NADP^+$. According to the proposed mechanism, in the absence of NADP, a mixed disulfide between a PDT thiol and the redox-

active cysteine is formed along with the formation of an FAD C4a-thiol charge-transfer interaction. Such a mechanism is also observed in glutathione reductase in the absence of NADP, with GSH as the reductant (*33*, *34*). In 2-KPCC, the CoM disulfide assumes a bench-like conformation, with the disulfide bridge forming the seat, while the sulfonates form the legs. One-half of this disulfide binds the same as the CoM part of 2-KPC, with ionic interactions between Arg365 and Arg56 of one subunit. The sulfonate from the other CoM extends a little away from these arginines to form interactions with carbonyl of Gln509 of the other subunit and water molecules but maintains proximity to Arg365, one of the oxygen atoms being 3.7 Å from NH_2. One of the oxygens of this sulfonate is 3.3 Å from Nϵ of His506 of the other subunit, which has Pro432 and Pro420 of the insertion loop on top and toward its front, respectively. During the course of the reaction leading to the formation of acetoacetate, the carboxylate moiety could be stabilized by the His and Gln of one of the subunits (Figure 6B and C). The interaction of the carboxylate with Arg365 concomitantly caused a weakening of the interaction between the CoM sulfonate and Arg365 and aided the release of CoM. The binding interactions of acetoacetate as compared to a CoM moiety can be speculated to be quite similar except in the vicinity of the carbonyl group, which could result in changes in the binding conformation conceivably favoring better stabilization of acetoacetate and destabilization of the CoM sulfonate−Arg binding interactions. The disulfide bond (S−S bond distance of 2.4 Å) of the CoM disulfide faces a hydrophobic pocket formed by Val77, Pro83, Val88, Pro136, and Met361 of one subunit and Met438, Phe442, Phe501, and Leu502 of the other subunit. One of the sulfurs of the disulfide bridge is 3.8 Å away from the sulfur of Cys82, which in turn is 2.2 Å from the Cys87 sulfur.

In our previous work, we have suggested that substrate binding induces conformational changes that result in the sequestration of the substrate to favor carboxylation over protonation. This was primarily based on the observation that the substrate access channel becomes much more restricted in the substrate-bound state in comparison to the native state. For the mixed-disulfide state in the current work, the substrate access channel is similar to that observed in the substrate-bound state; however, in the CoM-disulfide state, the channel widens slightly. This suggests an overall mechanism of the concerted stabilization of the developing charge of acetoacetate and the destabilization of the binding of substrates at the active site such that the electrostatic interactions at the active site that are generated during product formation are coupled to changes in the conformation of the N-terminal region of 2-KPCC that result in the opening of the active-site access, facilitating product release and enzyme turnover.

REFERENCES

1. Clark, D. D., Allen, J. R., and Ensign, S. A. (2000) Characterization of five catalytic activities associated with the NADPH:2-ketopropyl-coenzyme M [2-(2-ketopropylthio)ethanesulfonate] oxidoreductase/carboxylase of the *Xanthobacter* strain Py2 epoxide carboxylase system, *Biochemistry 39*, 1294−1304.
2. Westphal, A. H., Swaving, J., Jacobs, L., and de Kok, A. (1998) Purification and characterization of a flavoprotein involved in the degradation of epoxyalkanes by *Xanthobacter* Py2, *Eur. J. Biochem. 257*, 160−168.
3. Allen, J. R., and Ensign, S. A. (1997) Characterization of three protein components required for functional reconstitution of the epoxide carboxylase multienzyme complex from *Xanthobacter* strain Py2, *J. Bacteriol. 179*, 3110−3115.
4. Allen, J. R., and Ensign, S. A. (1997) Purification to homogeneity and reconstitution of the individual components of the epoxide carboxylase multiprotein enzyme complex from *Xanthobacter* strain Py2, *J. Biol. Chem. 272*, 32121−32128.
5. Ensign, S. A. (2001) Microbial metabolism of aliphatic alkenes, *Biochemistry 40*, 5845−5853.
6. Ensign, S. A., and Allen, J. R. (2003) Aliphatic epoxide carboxylation, *Annu. Rev. Biochem. 72*, 55−76.
7. Cleland, W. W., Andrews, T. J., Gutteridge, S., Hartman, F. C., and Lorimer, G. H. (1998) Mechanism of rubisco: The carbamate as general base. *Chem. Rev. 98*, 549−562.
8. Dowd, P., Hershline, R., Ham, S. W., and Naganathan, S. (1995) Vitamin K and energy transduction: A base strength amplification mechanism, *Science 269*, 1684−1691.
9. Janc, J. W., O'Leary, M. H., and Cleland, W. W. (1992) A kinetic investigation of phosphoenolpyruvate carboxylase from *Zea mays*, *Biochemistry 31*, 6421−6426.
10. Knowles, J. R. (1989) The mechanism of biotin-dependent enzymes, *Annu. Rev. Biochem. 58*, 195−221.
11. Swaving, J., de Bont, J. A., Westphal, A., and de Kok, A. (1996) A novel type of pyridine nucleotide-disulfide oxidoreductase is essential for NAD^+- and NADPH-dependent degradation of epoxyalkanes by *Xanthobacter* strain Py2, *J. Bacteriol. 178*, 6644−6646.
12. Nocek, B., Jang, S. B., Jeong, M. S., Clark, D. D., Ensign, S. A., and Peters, J. W. (2002) Structural basis for CO_2 fixation by a novel member of the disulfide oxidoreductase family of enzymes, 2-ketopropyl-coenzyme M oxidoreductase/carboxylase, *Biochemistry 41*, 12907−12913.
13. Williams, C. H., Jr. (1992) *Lipoamide Dehydrogenase, Glutathione Reductase, Thioredoxin Reducatse, and Mercuric Ion Reductase: A Family of Flavoenzyme Transhydrogenases*, Vol. 3, CRC Press, Boca Raton, FL.
14. Karplus, P. A., and Schulz, G. E. (1989) Substrate binding and catalysis by glutathione reductase as derived from refined enzyme: Substrate crystal structures at 2 Å resolution, *J. Mol. Biol. 210*, 163−180.
15. Pai, E. F., and Schulz, G. E. (1983) The catalytic mechanism of glutathione reductase as derived from X-ray diffraction analyses of reaction intermediates, *J. Biol. Chem. 258*, 1752−1757.
16. Schulz, G. E., Schirmer, R. H., Sachsenheimer, W., and Pai, E. F. (1978) The structure of the flavoenzyme glutathione reductase, *Nature 273*, 120−124.
17. Schiering, N., Kabsch, W., Moore, M. J., Distefano, M. D., Walsh, C. T., and Pai, E. F. (1991) Structure of the detoxification catalyst mercuric ion reductase from *Bacillus* sp. strain RC607, *Nature 352*, 168−172.
18. Mattevi, A., Schierbeek, A. J., and Hol, W. G. (1991) Refined crystal structure of lipoamide dehydrogenase from *Azotobacter vinelandii* at 2.2 Å resolution. A comparison with the structure of glutathione reductase, *J. Mol. Biol. 220*, 975−994.
19. Argyrou, A., and Blanchard, J. S. (2004) Flavoprotein disulfide reductases: Advances in chemistry and function, *Prog. Nucleic Acid Res. Mol. Biol. 78*, 89−142.
20. Allen, J. R., and Ensign, S. A. (1996) Carboxylation of epoxides to β-keto acids in cell extracts of *Xanthobacter* strain Py2, *J. Bacteriol. 178*, 1469−1472.
21. Jang, S. B., Jeong, M. S., Clark, D. D., Ensign, S. A., and Peters, J. W. (2001) Crystallization and preliminary X-ray analysis of a NADPH 2-ketopropyl-coenzyme M oxidoreductase/carboxylase, *Acta Crystallogr., Sect. D: Biol. Crystallogr. 57*, 445−447.
22. Leslie, A. G. W. (1992) *Joint CCP4 and ESF-EACBM Newsletter on Protein Crystallography Number 26*.
23. Collaborative Computational Project (1994) The CCP4 suite: Programs for protein crystallography, *Acta Crystallogr., Sect. D: Biol. Crystallogr. 50*, 760−763.
24. Brunger, A. T., Adams, P. D., Clore, G. M., DeLano, W. L., Gros, P., Grosse-Kunstleve, R. W., Jiang, J. S., Kuszewski, J., Nilges, M., Pannu, N. S., Read, R. J., Rice, L. M., Simonson, T., and Warren, G. L. (1998) Crystallography and NMR system: A new software suite for macromolecular structure determination, *Acta Crystallogr., Sect. D: Biol. Crystallogr. 54* (part 5), 905−921.
25. Jones, T. A., Zou, J. Y., Cowan, S. W., and Kjeldgaard, M. (1991) Improved methods for building protein models in electron density

maps and the location of errors in these models, *Acta Crystallogr., Sect. A: Found. Crystallogr. 47* (part 2), 110−119.
26. Laskowski, R. A., Moss, D. S., and Thornton, J. M. (1993) Main-chain bond lengths and bond angles in protein structures, *J. Mol. Biol. 231*, 1049−1067.
27. Guex, N., and Peitsch, M. (1997) SWISS-MODEL and the Swiss-PDB Viewer: An environemnt for comparative protein modeling, *Electrophoresis 18*, 2714−2723.
28. Christopher, J. A., Swanson, R., and Baldwin, T. O. (1996) Algorithms for finding the axis of a helix: Fast rotational and parametric least-squares methods, *Comput. Chem. 20*, 339−345.
29. *ACDlabs* (2003) Advanced Chemistry Development, Inc., Toronto, Ontario, Canada.
30. Alexander, R. S., Nair, S. K., and Christianson, D. W. (1991) Engineering the hydrophobic pocket of carbonic anhydrase II, *Biochemistry 30*, 11064−11072.
31. Fierke, C. A., Calderone, T. L., and Krebs, J. F. (1991) Functional consequences of engineering the hydrophobic pocket of carbonic anhydrase II, *Biochemistry 30*, 11054−11063.
32. Nair, S. K., and Christianson, D. W. (1993) Structural consequences of hydrophilic amino acid substitutions in the hydrophobic pocket of human carbonic anhydrase II, *Biochemistry 32*, 4506−4514.
33. Mannervik, B. (1973) A branching reaction mechanism of glutathione reductase, *Biochem. Biophys. Res. Commun. 53*, 1151−1158.
34. Rakauskiene, G. A., Cenas, N. K., and Kulys, J. J. (1989) A "branched" mechanism of the reverse reaction of yeast glutathione reductase. An estimation of the enzyme standard potential values from the steady-state kinetics data, *FEBS Lett. 243*, 33−36.

BI051518O